Computers and Electrical Engineering 126 (2025) 110478

Contents lists available at ScienceDirect

Computers and Electrical Engineering

journal homepage: www.elsevier.com/locate/compeleceng

Stress detection through wearable EEG technology: A signal-based approach

Rakesh Kumar Rai *, Dushyant Kumar Singh

Department of Computer Science & Engineering, MNNIT Allahabad, Prayagraj, 211004, UP, India

ARTICLE INFO

Keywords:
Stress detection
EEG signal
Wearable sensor
RLASSO
Hybrid Wavelet-Short-Time Fourier Transform
GAN

ABSTRACT

Accurate and non-invasive stress detection is critical for mental health monitoring and early intervention. Among various physiological signals, electroencephalography (EEG) offers a unique advantage as it captures direct neural activity, making it more responsive to cognitive and emotional stress compared to peripheral markers like heart rate or skin conductance. In this work, we propose a novel EEG-based stress detection framework that combines Fuzzy Attention-based Fully Convolutional Network (FA-FCN) for dynamic signal segmentation, Hybrid Wavelet-Short-Time Fourier Transform (HW-STFT) for rich time–frequency feature extraction, Recursive LASSO (RLASSO) for optimal feature selection, and an Adam-Optimized Sequential Generative Adversarial Network (AOS-GAN) for robust classification. Each component is specifically designed to address the limitations of existing methods FA-FCN enhances signal relevance by focusing on stress-related EEG regions, while HW-STFT captures transient frequency shifts with high resolution. RLASSO improves computational efficiency by reducing dimensionality, and AOS-GAN enhances classification in imbalanced conditions using adversarial learning. Our model achieves an accuracy of 94%, significantly outperforming other state-of-the-art methods, which typically report accuracies around 85%–89%. This demonstrates the model's strong potential for real-world deployment in high-stress environments such as emergency response, cognitive workload monitoring, or workplace mental health systems. Future work will focus on validating this approach across larger and more diverse EEG datasets, enabling real-time deployment on edge devices, and exploring multimodal integration with other physiological signals for holistic stress assessment.

1. Introduction

Stress, a common aspect of daily life, often involves high pressure and remains a significant risk factor for cardiovascular events [1–3]. It is classified into eustress ("good stress") and distress ("bad stress") [4–6]. Distress can impair work performance and increase risks of psychological conditions like anxiety and physiological conditions like hypertension, with symptoms such as anxiety, headaches, and poor concentration [7]. Effective stress management is crucial due to its link to chronic health issues like depression [8] and its adverse effects on health, including insomnia, weakened immunity, migraines, and severe illnesses such as diabetes, cancer, and heart disease [9,10]. Continuous monitoring of individuals at high risk is essential to prevent health issues. The Internet of Medical Things (IoMT), a network of interconnected sensors and devices, plays a crucial role in stress detection by collecting, transmitting, and analyzing stress data, thus enhancing remote monitoring, preventive care, and workflow efficiency in healthcare [11]. Wearable technology, which enables real-time stress monitoring through sensors that detect physiological

* Corresponding author.
E-mail addresses: rakesh.2021rcs54@mnnit.ac.in (R.K. Rai), dushyant@mnnit.ac.in (D.K. Singh).

https://doi.org/10.1016/j.compeleceng.2025.110478
Received 17 December 2024; Received in revised form 20 April 2025; Accepted 25 May 2025

indicators such as body temperature, heart rate, and blood pressure, has become increasingly popular [12,13]. These affordable and user-friendly sensors measure physiological responses to stress.

Traditional stress detection methods using physiological signals such as Heart Rate Variability (HRV), Electrocardiography (ECG), and Galvanic Skin Response (GSR) have shown promise in monitoring autonomic responses to stress. However, these signals are often influenced by external factors, such as temperature, movement, or hydration, leading to inconsistent and noisy measurements. Moreover, they provide only indirect assessments of mental or emotional stress, limiting their reliability in cognitively demanding environments. In contrast, EEG signals offer a direct window into brain activity, enabling more precise identification of stress-induced neural patterns.

Our study focuses on stress detection using wearable sensors, specifically using EEG signals. EEG records brain electrical activity via scalp sensors connected to an EEG machine or amplifier. The EEG signal is collected from wearable sensors, preprocessed with filtering and artifact removal, and segmented using a fuzzy attention-based fully convolutional network (FA-FCN). EEG-based methods offer higher sensitivity in detecting mental stress, yet challenges remain in feature selection and segmentation. This study addresses these gaps by proposing an optimized feature extraction and classification approach to improve detection accuracy and generalizability. To improve stress detection accuracy, this study leverages advanced deep learning techniques. FA-FCN enhances EEG signal segmentation, Hybrid Wavelet Short-Time Fourier Transform (HW-STFT) refines feature extraction, and Recursive Least Absolute Shrinkage and Selection Operator (RLASSO) optimizes feature selection. Finally, Adam-optimized sequential generative adversarial network (AOS-GAN) is used for robust classification.

1.1. Motivation

Mental stress has become a critical public health concern, contributing to various cognitive, emotional, and physical disorders. Traditional methods of stress detection, such as questionnaires or behavioral observation, are often subjective, non-continuous, and unsuitable for real-time monitoring. EEG-based analysis offers a promising alternative by providing direct, objective, and real-time insights into brain activity associated with stress. However, existing EEG-based systems often suffer from limited accuracy, high noise sensitivity, and poor generalization across individuals. This research is motivated by the need for a robust, efficient, and scalable EEG-based stress detection system to overcome these challenges and move closer to real-world applications. Common issues in existing research include:

1. **Limited Generalization Due to Insufficient Training Data:** Many existing stress detection models struggle to generalize across individuals and stress scenarios due to limited and homogeneous training datasets, which negatively impacts accuracy.
2. **Suboptimal Feature Selection:** Traditional methods often fail to identify the most informative EEG features. Including irrelevant or redundant features introduces noise, which reduces classification performance and masks critical stress-related patterns.
3. **Ineffective EEG Segmentation:** Current approaches face difficulty in capturing subtle temporal dynamics of stress responses within high-dimensional EEG data. Poor segmentation hinders the model's ability to detect transient patterns, which are essential for accurate stress recognition.

This study aims to develop a reliable method for diagnosing and recognizing mental stress using EEG data from wearable sensors. The objectives include:

1. Detecting stress in individuals using wearable sensors to enhance their quality of life.
2. Predicting stress levels by analyzing physiological (EEG) data during stressful situations.
3. Developing a non-invasive, real-time system for reliable and accurate stress measurement.
4. Analyzing EEG data to extract relevant features for stress identification using advanced machine learning and AI algorithms.

1.2. Research contributions

This study presents a novel approach to EEG-based stress detection through wearable sensors, addressing key limitations in existing methods. The primary scientific contributions of this work are:

1. **Understanding Stress-Induced EEG Changes:** This study deepens scientific insight into how mental stress affects brain activity by analyzing EEG patterns linked to stress-related neural responses.
2. **Hybrid Feature Extraction and Selection:** We propose a novel HW-STFT + RLASSO framework that captures time–frequency dynamics and performs sparse feature selection, enhancing interpretability and cross-subject generalization.
3. **Robust Classification via Adversarial Learning:** The AOS-GAN classifier improves stress detection by learning complex nonlinear EEG patterns and reducing dependence on large labeled datasets.
4. **Real-World Applicability:** The system supports integration into wearable devices for real-time, non-invasive stress monitoring, with potential applications in mental health, workplace stress tracking, and personalized wellness.
5. **Validated Performance:** Experimental results show that the proposed model achieves 94% accuracy, outperforming existing approaches and providing a strong foundation for future EEG-based stress detection research.

The remainder of this paper covers related works, problem definition, proposed methodology, experimental analysis, and conclusion.

Table 1
Related works.

Ref.	Objectives	Methods used	Limitations
[14]	Detect brain waves for stress assessment.	SVM, RF, DT, LR, KNN	High processing power needed
[15]	Use ensemble decomposition for mental state classification.	Wavelet, DWT, TQWT	Inaccurate classification
[16]	Recognize psychological states from EEG.	CNN-Bi-LSTM-Attention	Requires large labeled data
[17]	EEG-based MDD screening using ML/DL and mRMR.	mRMR, SVM, KNN, DT	Info loss in feature selection
[18]	EEG-based MDD detection method.	LNR, SVM, PCC	Overfitting in feature selection
[19]	Classify depression using EEG features.	SVM, LDA, NB, KNN, DT	Multimodal data handling issues
[20]	EEG-based emotion recognition.	LSTM-CNN hybrid	Minority class recognition challenges
[21]	Analyze depression using ML on EEG.	SVM, RF	Poor performance on minority class
[22]	Classify mental pressure (MP) using EEG.	CNN	Hard to generalize to new stresses
[23]	Determine stress via CNN + DWT.	BiLSTM	Handling variable length data
[24]	Improve emotion recognition accuracy via EEG.	SHGO	Difficult to interpret results
[25]	Emotion AI using valence recognition on EEG.	Hjorth, PSD, zero-crossing SVM, KNN	EEG scaling/normalization issues
[26]	Detect depression from EEG signals.	RF, XGBoost, 1D CNN	Fails with complex EEG data
[27]	Stacking-ensemble for emotion classification via EEG.	RF, GBC, LightGBM	Poor on varied/unknown data
[28]	EEG brain mapping for emotion detection.	GRU, CNN	Fails to capture long-term dependencies
[29]	Extract depressive emotions using DL on EEG.	CNN, Bi-LSTM	High computational complexity
[30]	Analyze emotions using EEG from GAMEEMO dataset.	BiLSTM	Overfitting problems
[31]	EEG-based stress classification.	BiLSTM	Requires balancing for unbalanced datasets
[32]	End-to-end RA2–3DCNN for emotion classification from EEG.	RA2–3DCNN	Complexity, overfitting issues

2. Related works

Previous EEG-based research on stress detection and mental state classification has revealed several challenges. Study [14] noted difficulties in processing high-dimensional EEG data, which required substantial computational resources. In [15], Discrete Wavelet Transform (DWT) struggled with artifact management, affecting stress classification accuracy. The CNN-Bi-LSTM attention model in [16] faced issues due to the lack of labeled data. Using Minimum Redundancy Maximum Relevance (mRMR) in [17] led to information loss and poor feature selection. Recursive Feature Elimination (RFE) in [18] was found to experience overfitting with high-dimensional data. Naive Bayes in [19] had trouble handling multimodal data for stress classification. LSTM-CNN hybrid models in [20] struggled with imbalanced datasets, while Random Forest (RF) showed bias towards dominant classes in [21]. CNNs overfitted in cross-session mental pressure classification [22], and CNN-BiLSTM-GRU models had issues with variable-length sequences [23]. SHGO's optimization in [24] was challenging to interpret. Support Vector Machines (SVMs) in [25] were sensitive to input ranges, and K-Nearest Neighbors (KNN) had class-size sensitivity. RF underperformed on complex EEG datasets for depression detection in [26], and LightGBM performed poorly with unseen data in [27]. GRUs in CNN-GRU models failed to capture long-term dependencies [28], while CNN-Bi-LSTM models faced computational and equipment issues [29]. Bi-LSTM networks in [30] overfitted with small datasets, and BiLSTM models in [31] required oversampling/undersampling. Finally, RA2–3DCNNs in [32] were prone to overfitting with small datasets (see Table 1).

The work [33] presents MuLHiTA, a multiclass stress detection framework using a multi-branch BiLSTM network with hierarchical temporal attention. It captures both interslice and interslice temporal dependencies through parallel branches and specialized attention modules. Another paper [34] proposes a hybrid DL model based on discrete wavelet transform (DWT) that combines CNN and bidirectional long short-term memory (CNN-BLSTM) to assess human stress levels. It is observed that the proposed approaches struggles with new and unknown stress patterns and does not generalize well to novel stress patterns.

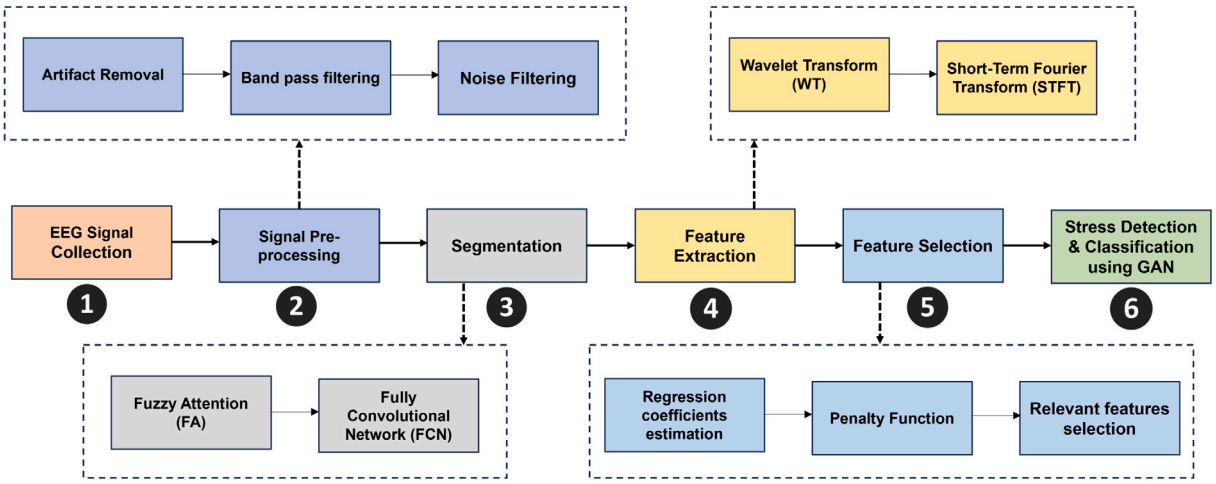

Fig. 1. Proposed architecture. This figure illustrates the overall pipeline of the proposed EEG-based stress detection framework, integrating signal preprocessing, segmentation, feature extraction, feature selection, and classification. The key innovation is the use of hybrid feature extraction (HW-STFT) and adversarial learning (AOS-GAN) to improve stress detection accuracy while maintaining computational efficiency for real-time applications.

The article [35] offers a novel approach to EEG signal detection for mental stress. The EEG data was split up, and characteristics based on entropy were extracted using the stationary wavelet transform. The work [36] proposes a metaheuristic fuzzy inference system (fMFiS-L) for emotion-based stress detection using EEG data and Likert scale ratings, with a focus on Internet of Medical Things (IoMT) and smart home settings. However, it suffers from class imbalance, as the modified fusion method tends to misclassify the minority-stressed group. The study [37] proposes a mix of statistical importance (CIS)-based "K-Nearest Oracles Union" (KNORA-U) and "Dynamic Ensemble Selection" (DES) models to assess human stress levels. Statistically based feature selection in stress detection, as statistical measurements may not accurately represent complex stress patterns.

3. Proposed method

The proposed work focuses on using wearable sensors and EEG signals to identify mental stress, which can have serious adverse effects on both mental and physical health. Therefore, detecting stress is the main objective. Fig. 1 illustrates the proposed architecture.

The primary processes involved in this approach are as follows:

1. Signal collection
2. Signal Preprocessing
3. Segmentation
4. Feature extraction
5. Feature selection
6. Stress detection and classification

3.1. Signal collection

Wearable electroencephalogram (EEG) sensors, typically placed on specific scalp areas, detect brain activity to identify stress. These sensors, which are made of metal discs or embedded in a cap, are attached using conductive paste or gel and then connected to an EEG amplifier or data collection system. This paper utilizes the Mental Arithmetic Task dataset from PhysioNet, which comprises EEG recordings taken before and during mental tasks. The dataset is divided into three subsets: training for model training, validation (without labels) for adjusting model parameters and evaluating performance, and testing to assess the model's ability to predict stress on new, unseen EEG data.

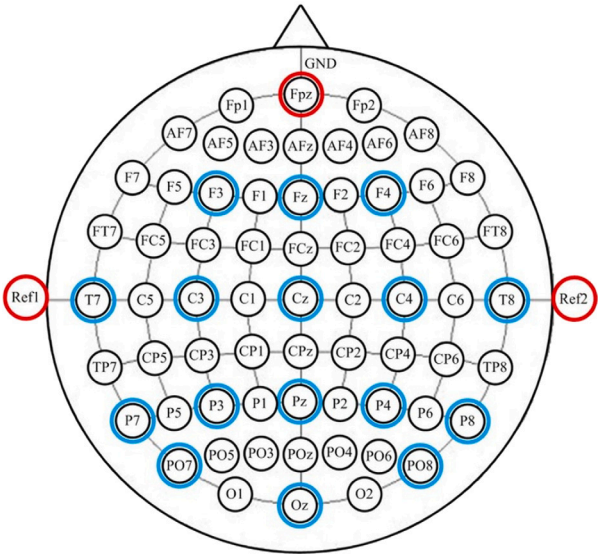

Fig. 2. Electrode positions for EEG recording. (16 EEG recording electrodes, one ground electrode, and two references). [38].

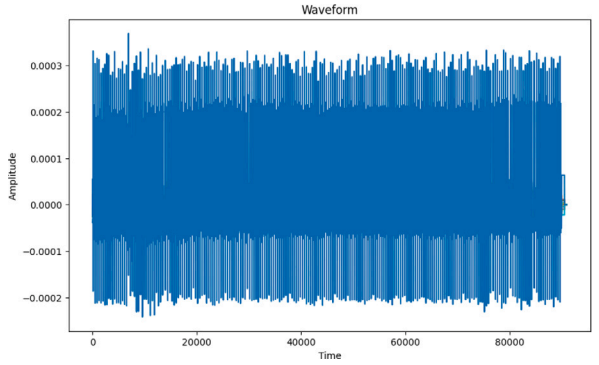

Fig. 3. Raw EEG Signal in Time Domain. A sample of an unprocessed EEG signal collected from a subject before preprocessing. The presence of artifacts (e.g., muscle movement, electrical noise) is evident, necessitating careful filtering to ensure accurate stress classification.

3.1.1. EEG signal

The brain's millions of neurons communicate via electrical impulses, which are captured as EEG signals (Fig. 2). Artifacts, such as electrical grids and muscle activity, can disrupt these signals, necessitating expert analysis. EEG frequency varies with mental state: alpha waves (8–12 Hz) during relaxation, beta waves (13–40 Hz) during attention, delta waves (0–4 Hz) during deep sleep, and theta waves (4–7 Hz) in newborns or during specific activities. The raw EEG signal of one of the subjects under study is shown in Fig. 3

3.2. Signal preprocessing

Before feature extraction, the raw EEG data undergoes preprocessing, including filtering and artifact removal. Bandpass and noise (notch) filters reduce noise and interference, improving the signal-to-noise ratio and focusing on stress-related frequency components. Artifact removal eliminates non-brain-related artifacts, like muscle activity or eye blinks, ensuring that the EEG data

accurately represents stress-related neuronal activity. These preprocessing steps enhance data quality, leading to more accurate and reliable stress detection.

3.2.1. Artifact removal

The process of eliminating or adjusting artifacts without affecting the underlying, relevant biological signal is known as "artifact removal". The artifact-contaminated section can be rejected or canceled as a straightforward method of reducing the impact of artifacts once they have been detected. Since both of these processes overlap in the temporal domain, this approach ultimately results in the loss of crucial information, in addition to removing artifacts and signals of significance.

3.2.2. Band pass filtering

A band-pass filter allows signals within a specific frequency range to pass through while attenuating unwanted frequencies outside this range. In this study, we apply a band-pass filter with a frequency range of 7–30 Hz to remove irrelevant and noisy components from the EEG signal. By applying a 7–30 Hz band-pass filter, we achieve the following:

- *Elimination of Low-Frequency Artifacts (<7 Hz):* Eye Blinks and Movements (<4 Hz): These generate slow drifts in the EEG signal, which can interfere with stress-related brain activity. Cardiac activity (1–1.5 Hz) produces rhythmic artifacts that can distort EEG readings. Slow fluctuations (0–1 Hz) are removed due to factors such as sweat, electrode impedance, and environmental interference.
- *Removal of High-Frequency Artifacts (>30 Hz):* Facial and scalp muscle movements introduce high-frequency noise (>30 Hz). While a notch filter is specifically used for powerline noise, the band-pass filter also helps in minimizing residual high-frequency noise (~50/60 Hz).
- *Preservation of Stress-Related Brain Activity (7–30 Hz)*: Theta Waves (4–7 Hz), which are associated with emotional processing, relaxation, and cognitive engagement, should be preserved. Additionally, Alpha Waves (8–12 Hz), which are associated with mental workload and stress levels, and Beta Waves (13–30 Hz) correlate with heightened alertness, anxiety, and stress-induced cognitive load.

A Butterworth filter is commonly used due to its smooth response and minimal signal distortion. The band-pass filter is applied using the Butterworth filter equation:

$$H(f) = \frac{1}{\sqrt{1 + (\frac{f}{f_c})^{2N}}} \tag{1}$$

where $H(f)$ is the frequency response, f_c is the cutoff frequency (7 Hz and 30 Hz in this case), and N is the filter order (higher values give a sharper transition). After applying the band-pass filter, we normalize the EEG signal for consistency using standard normalization:

$$X_{norm} = \frac{X - \mu}{\sigma} \tag{2}$$

where X is the band-pass filtered EEG signal, μ is the mean of the signal, and σ is the standard deviation.

3.2.3. Noise filters

Removing the power line interference (PLI) fundamental frequency is often sufficient, as most biosignals have maximum frequencies up to 100 Hz. Notch filtering eliminates both the signal component and PLI at the fundamental frequency. However, designing a notch filter requires prior knowledge of the notch frequency, which may vary in practice. This variation can result in the unintended removal of essential signal components, such as the gamma rhythm in EEG recordings, in addition to the PLI.

3.3. Segmentation

EEG signals are recorded as continuous waves of electrical activity. However, analyzing them as a whole can be overwhelming. In EEG signal processing, segmentation is an important technique used to break down the continuous stream of brain signals into smaller, meaningful segments for analysis. In our approach, we use a Fuzzy Attention-based Fully Convolutional Network (FA-FCN) to segment EEG signals. This technique automatically identifies important sections of the signal, ensuring that only relevant brain activity is analyzed. The preprocessed EEG signals are split into 50 different segments. By using FA-FCN, the model can better understand which parts of the EEG signal contain stress-related activity, making the stress detection process more efficient and reliable. Fig. 4 shows one of the segments of the preprocessed EEG signal. The details of the segmentation process and the FA-FCN are described below:

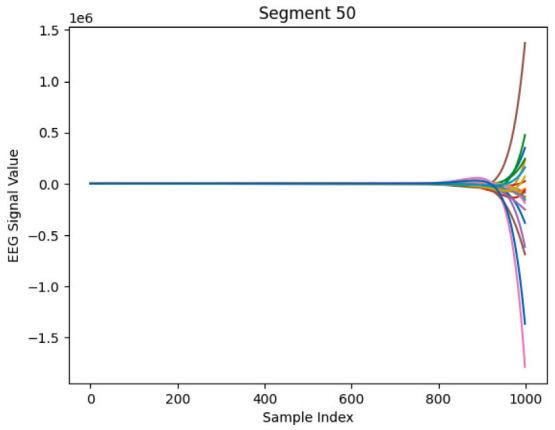

Fig. 4. One of the Segments of the pre-processed EEG Signal. One of the 50 segments obtained from the EEG signal using the Fuzzy Attention-Based Fully Convolutional Network (FA-FCN). Proper segmentation enables the model to capture stress-related patterns more effectively by isolating relevant brainwave activity.

3.3.1. Fuzzy attention

Fuzzy logic employs concepts such as membership functions, replicating the human brain's uncertain manner of thought and reasoning to address the relationships and associations between fuzzy sets. When signal segmentation is to be controlled by downsampling, the fuzzy attention module is placed on the feature channel in the encoding stage and on the spatial area in the decoding stage. This allows the relative significance of the features to be recalculated.

Fuzzy Channel Attention Module in the Up-Sampling Layer: The feature channels of the up-sampling layer are where the fuzzy attention module is located. The fuzzy layer's embedding position must be established first. Let R, G, U, and B be the dimensions of the input data. Conduct two complete connection procedures in the feature channel's attention module. In the first complete connection, there are $R \times 1 \times 1 \times (B/16)$ neurons, while in the second, there are $R \times 1 \times 1 \times B$ neurons. Depending on the degree of membership that fuzzy logic creates, the weight of the correlation parameter between the output's characteristic channels may be altered. The output of the first complete connection layer and the second entire connection layer provides input to the fuzzy layer. The fuzzy mechanism layer surrounds the two complete connection layers. The membership function of the fuzzy layer, an S-type function with a fuzzy membership feature, is given by Eq. (3).

$$\mu(z) = \frac{1}{1 + m^{pz+q}} \tag{3}$$

The S-type membership function calculates values from 0 to 1, with higher certainty at the edges and lower certainty at the center. Two uncertainty thresholds guide this process, reflecting lower confidence in mid-range values and higher confidence in extremes. High-certainty weights are enhanced while low-certainty weights are simplified. Reapplying the S-type function results in a membership value of 0.5, indicating limited certainty. An affine transform adjusts weights, with larger values indicating better predictability. Batch normalization enhances target region differentiation, and the fuzzy channel attention module, when combined with the downsampling module, further improves this capability.

The Fuzzy Spatial Attention Module in the up-sampling layer assigns weights to pixels based on membership uncertainty, increasing weights for low-uncertainty pixels and decreasing them for high-uncertainty ones. This module, placed after the final convolution and before numerical multiplication with the original feature map, improves precision by combining deep features' up-sampling with shallow data's down-sampling. It enhances the up-sampling process by reducing image detail loss and expanding the receptive field.

3.4. Feature extraction

To convert raw EEG signals into useful features for stress detection, feature extraction is a crucial step. Extracted features simplify the understanding and communication of stress results compared to raw data. Key stress-related EEG features include frequency bands (alpha, beta, delta, theta, gamma), spectral power, event-related potentials (ERPs), and synchronization patterns. This work proposes using the Hybrid Wavelet-Short-Time Fourier Transform (HW-STFT) for feature extraction because traditional methods struggle with analyzing signals that change over time. HW-STFT combines two techniques:

1. *Wavelet Transform:* Captures both high and low-frequency changes, useful for detecting rapid brain activity changes.

2. *Short-Time Fourier Transform (STFT):* Provides detailed time–frequency analysis, helping track how stress-related brain waves evolve over time.

This combined method allows us to extract key stress-related features while maintaining accuracy.

Algorithm 1 Proposed Method for EEG Stress Detection.

Step 1: Collecting and Cleaning EEG Signals
function BANDPASS_FILTER($x(t)$, f_{low}, f_{high}, f_s, N):
  $f_{\text{Nyquist}} \leftarrow 0.5 \times f_s$
  $f_{\text{low\_norm}} \leftarrow \frac{f_{\text{low}}}{f_{\text{Nyquist}}}$
  $f_{\text{high\_norm}} \leftarrow \frac{f_{\text{high}}}{f_{\text{Nyquist}}}$
  $(b, a) \leftarrow$ BUTTERWORTH_BANDPASS_FILTER($f_{\text{low\_norm}}, f_{\text{high\_norm}}, N$)
  return LFILTER($b, a, x(t)$)
function PREPROCESS_EEG(X_{raw}):
  return BANDPASS_FILTER($X_{\text{raw}}, 7, 30, 256, 5$)
Step 2: Segmenting the Signal
function SEGMENT_SIGNAL($X_{\text{preprocessed}}, L_{\text{seg}}$):
  Segments $\leftarrow \emptyset$
  for $k = 0$ **to** $\text{len}(X_{\text{preprocessed}}) - L_{\text{seg}}$ **by** L_{seg}:
    $x_k \leftarrow X_{\text{preprocessed}}[k : k + L_{\text{seg}}]$
    if $\text{len}(x_k) = L_{\text{seg}}$:
      Segments $\leftarrow$ Segments $\cup \{x_k\}$
  return Segments
Step 3: Feature Extraction using HW-STFT
function WAVELET_TRANSFORM($x(t)$):
  $\Psi(t) \leftarrow$ Wavelet Function
  $C(a, b) \leftarrow \int x(t)\Psi\left(\frac{t-b}{a}\right) dt$
  return C
function SHORT_TIME_FOURIER_TRANSFORM($x(t)$, f_s):
  $\{f, \tau, Z\} \leftarrow \text{STFT}(x(t), f_s, \text{window length } 128)$
  return $|Z|$
function EXTRACT_FEATURES(Segments):
  Features $\leftarrow \emptyset$
  for each x_k **in** Segments:
    $C_{\text{wavelet}} \leftarrow$ WAVELET_TRANSFORM(x_k)
    $S_{\text{STFT}} \leftarrow$ SHORT_TIME_FOURIER_TRANSFORM(x_k)
    $f_{\text{combined}} \leftarrow \text{concatenate}(C_{\text{wavelet}}, \text{flatten}(S_{\text{STFT}}))$
    Features $\leftarrow$ Features $\cup \{f_{\text{combined}}\}$
  return Features
Step 4: Feature Selection with RLASSO
function FEATURE_SELECTION(Features, Y, α):
  $\mathcal{L} \leftarrow$ LASSO Regression(α)
  $\mathcal{L} \leftarrow$ Fit Model($\mathcal{L}$, Features, Y)
  return $F_{\text{selected}} = \text{Features}[:, \text{non-zero coefficients in } \mathcal{L}]$

The "wavelet transform" (WT) is a potent contemporary method for time–frequency analysis of non-stationary data, including EEGs. WT is a group of decomposition functions of the correlation between the signal and the dilation and the shifting and dilation of a single, specialized function called the mother wavelet function (MWT). When it comes to time–frequency analysis for non-stationary data, the wavelet transform (WT) is a valuable processing technique that has been developed. For a signal, the continuous WT (CWT) is defined in Eq. (4):

$$\text{CW}_T(x, y; z) = \frac{1}{\sqrt{|x|}} \int z(s)\Psi\left(\frac{s-y}{x}\right) ds \tag{4}$$

where (s) is called the Mother Wavelet Function (MWT), while x and y (x, y IR) are dilation and translation parameters, respectively. Since the variable x functions as the frequency's reverse, a smaller value corresponds to a shorter mean wavelength in the time domain and a higher central frequency in the spectrum. This formula may also be understood as the signal projection when examining family functions that are created from the mother wavelet function according to the following Eq. (5):

$$\Psi_{x,y}(s) = \frac{1}{\sqrt{x}}\Psi\left(\frac{s-y}{x}\right) \tag{5}$$

The wavelet transform is reversible if the mother wavelet function is selected carefully, and the signal may be reconstructed using the following Eq. (6) after analysis and the synthesis method:

$$z = K\psi^{-1} \int_{-\infty}^{+\infty} \int_{-\infty}^{+\infty} \frac{1}{x^2} \langle z, \psi_{x,y} \rangle \psi_{x,y}\, dx\, dy \tag{6}$$

Since the calculation can only be performed numerically and convergence may be too slow, this approach is only feasible in principle. The coefficient can be expressed as the following Eq. (7) if it exists:

$$K_\psi = 2\pi \int_{-\infty}^{\infty} |\Psi(\omega)|^2 \frac{1}{\omega}\, d\omega \tag{7}$$

The mother wavelet function's admissibility requirement is equally responsible for the current state of this coefficient. The following Eq. (8) is used to represent this condition.

$$\int_0^{\infty} |\Psi(\omega)|^2 \frac{1}{\omega}\, d\omega = \int_{-\infty}^{0} |\Psi(\omega)|^2 \frac{1}{\omega}\, d\omega > \infty \tag{8}$$

This relationship is often linked to the moderately restrictive condition found in Eq. (9), which states that the mother wavelet function can have an average value of zero.

$$\int_{-\infty}^{\infty} \Psi(s)\, dt = 0 \tag{9}$$

Discrete Wavelet Transform (DWT) is often required for Wavelet Transform (WT) applications in engineering disciplines. DWT requires less computing time than CWT and is non-redundant. The discrete values of the parameters x and y define the Discrete Wavelet Transform (DWT).

$$\mathrm{DWT}_{p,q}(z) = x_0^{-p/2} \int z(s) \Psi \left(x_0^{-p/2} s - q y_0 \right) dt \tag{10}$$

where p and q (p, q Z) in Eq. (10) indicate frequency and time localization, respectively.

The Short-Time Fourier Transform is used to analyze the time–frequency domain link of non-stationary signals. The frequency content of a sliding, short-time windowed signal is calculated. Additionally, we utilized a short time window length, S, to account for signal attenuation at the window margins and the overlap length, L, in conjunction with the Q sample intervals of the temporal window. Discovering that Q = S-L is simple. The ith trial EEG signal z(n) has the STFT characteristics, where h is the EEG data channel and is the STFT matrix of the jth channel. The z(n) is given trailing zeros to add to its length of 1024 after the number of rows, R, is set to 1024 points. The number of columns C is determined by:

$$C = \left\lfloor \frac{T_z - R}{S - R} \right\rfloor \tag{11}$$

where The length of the ith trial EEG signal, and $\lfloor \cdot \rfloor$ are the floor function.

The mth element of x_i is:

$$f_m = \sum_{n=-\infty}^{\infty} z(n) u(n - mQ) e^{-j2\pi f n} \tag{12}$$

where f_m is the DFT of the windowed EEG signal centered about time Mq, $u(n)$ is the window function of length S and given as follows:

$$u(n) = \frac{I_0\left(\beta \sqrt{1 - \left(\frac{n + \left(-\frac{S}{2} \right)}{\frac{S}{2}} \right)^2} \right)}{I_0(\beta)}, \quad 0 \le n \le S \tag{13}$$

where $I_0(\cdot)$ is the zeroth-order modified Bessel function of the first kind.

$$I_a(w) = \left(\frac{w}{2} \right)^a \sum_{\epsilon=0}^{\infty} \frac{\left(\frac{w^2}{4} \right)^\epsilon}{\epsilon! \Gamma(a + \epsilon + 1)} \tag{14}$$

where a in Eq. (12) is the order of the modified Bessel function of the first kind. $\Gamma(\cdot)$ is the Gamma function.

$$\Gamma(w) = \int_0^{\infty} e^{-t} t^{w-1}\, dt, \quad w \in \mathbb{R} > 0 \tag{15}$$

The "Hybrid Wavelet and Short-Time Fourier Transform" (HW-STFT) approach is employed in this study to enhance EEG feature extraction. The short-time Fourier transform provides temporal information by examining signal changes over time, whereas the wavelet transform captures both high- and low-frequency components. By incorporating these two transformations, the HW-STFT method enhances stress detection feature extraction by providing a more comprehensive description of EEG data. It is possible to construct effective EEG-based stress detection systems by comprehending the complex dynamics of stress-related brain activity.

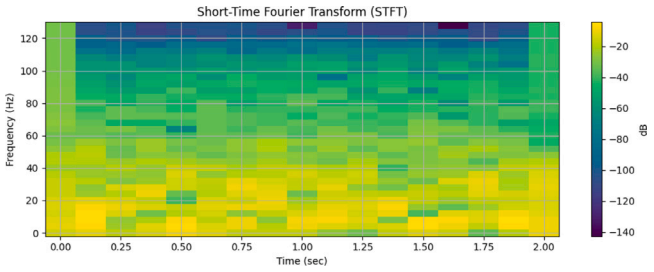

Fig. 5. Signal transformed using Hybrid Wavelet and Short-Time Fourier Transform (HW-STFT). This transformation captures both time–frequency characteristics and localized frequency variations in EEG signals. The HW-STFT method enhances the ability to detect stress-induced neural oscillations by preserving both high and low-frequency components.

EEG signals are inherently non-stationary and time-dependent, making fixed-window methods like Discrete Fourier Transform (DFT) or pure Short-Time Fourier Transform (STFT) insufficient for capturing complex and transient neural patterns. While Wavelet Transform (WT) offers multi-resolution analysis, it can miss short bursts of frequency shifts that are critical in stress-related transitions. HW-STFT combines the localized time–frequency analysis of STFT with the multi-scale capabilities of WT, enabling a more precise capture of stress-induced EEG dynamics. The Signal transformed using HW-STFT is shown in Fig. 5.

3.5. Feature selection

In EEG-based stress detection, feature extraction is followed by feature selection, which retains only the most relevant information while removing redundant or irrelevant features. This step enhances both the accuracy and computational efficiency of the classification model by reducing overfitting and focusing on stress-related EEG patterns. In this study, we employ the Recursive Least Absolute Shrinkage and Selection Operator (RLASSO) for feature selection. RLASSO extends the LASSO technique by iteratively refining feature importance, promoting sparsity, and ensuring that only the most significant EEG features are retained. This simplifies the model, lowers data complexity, and improves its ability to distinguish between stress and non-stress conditions.

Algorithm 2 Working procedure of LASSO algorithm.

Input: Data $\{\dots\}$; Sampling ratio $\in (0, 1)$;
Number of randomizations $Z \in \mathbb{Z}^+$; threshold $R \in \mathbb{R}^+$
Output: Relevant features f
for $h = 1, 2, \dots, Z$ **do**
    Data = sampling with substitution from ratio-based data
    Perform LASSO-based feature selection using EEG data
end for
Frequency of selection of each feature is calculated according to $h = 1, 2, \dots, Z$
Return f: the set of features selected most frequently

Fig. 6 shows the t-SNE feature projection of EEG data before and after RLASSO feature selection. The t-SNE projection reveals a wider and more mixed distribution of stress and non-stress classes prior to RLASSO, whereas after RLASSO, the features form tighter and more distinguishable clusters. This suggests that RLASSO enhances class separability by removing irrelevant or redundant features.

3.6. Stress detection and classification

This study uses the Adam-optimized sequential generative adversarial network (AOS-GAN) for stress detection and classification. While GANs face challenges such as data requirements, privacy concerns, training instability, and interpretability issues, AOS-GAN effectively addresses these problems. It identifies stress from diverse sources, including EEG, physiological signals, text, and audio. The AOS-GAN's optimization and sequential approach manage stress detection well, and once detected, it provides feedback to promote self-help techniques like yoga, meditation, exercise, and a balanced diet for stress reduction and a healthy lifestyle.

The traditional models, such as SVM, Random Forests, or even standard CNNs, often require balanced datasets and large amounts of labeled data, which are not always available in physiological signal processing. AOS-GAN addresses these limitations by employing adversarial learning to generate realistic EEG-like samples, thereby effectively reducing class imbalance and enhancing generalization. The Adam optimizer further enhances training stability and convergence speed. This combination enables the model to learn complex, nonlinear representations of stress patterns with increased robustness, as demonstrated by its superior performance across multiple evaluation metrics.

Adam is a robust adaptive optimization algorithm that is an alternative to traditional stochastic gradient descent. It is computationally efficient, with minimal memory requirements, and dynamically adjusts the learning rate for each parameter. Adam combines momentum and RMSProp techniques, utilizing the exponential moving averages of the gradient (β_1) and the squared

gradient (β_2), enabling it to traverse complex, high-dimensional parameter spaces effectively. This adaptability enables Adam to quickly find optimal solutions, making it well-suited for tasks such as stress classification. Parameter updates are performed using Eqs. (16) to (19).

$$e_z = \beta_1 e_{z-1} + (1-\beta_1) y_z \tag{16}$$

$$s_z = \beta_2 s_{z-1} + (1-\beta_2) y_z^2 \tag{17}$$

$$\hat{e}_z = \frac{e_z}{1-\beta_1^z} \quad \hat{S}_z = \frac{s_z}{1-\beta_2^z} \tag{18}$$

$$\theta_{z+1} = \theta_z - \eta \frac{\hat{e}_z}{\sqrt{\hat{S}_z} + \epsilon} \tag{19}$$

where β_1 is the exponential decay rate. The default values for β_1 and β_2 are 0.9 and 0.999, respectively. $\hat{e}_z$ and $\hat{S}_z$ are the correction biases for e_z and S_z respectively.

Algorithm 3 Stress Detection and Classification using GAN.

Step 5.1: Generator Class
class GENERATOR:
  Initialize generator network layers
  function $g(z)$:
    return forward pass through generator network
Step 5.2: Discriminator Class
class DISCRIMINATOR:
  Initialize discriminator network layers
  function $d(x)$:
    return forward pass through discriminator network
Step 5.3: Build GAN
function BUILD_GAN(g, d):
  $G \leftarrow$ Sequential(g, d)
  return G
Step 5.4: Train GAN
function TRAIN_GAN($G, g, d, F_{\text{selected}}, N_{\text{epochs}}, M_{\text{batch}}$):
  for each epoch = 1 **to** N_{epochs}:
    for each batch in 0 to len(F_{selected}) **by** M_{batch}:
      $x_{\text{real}} \leftarrow$ batch from F_{selected}
      $z_{\text{noise}} \sim \mathcal{N}(0,1)$ of size M_{batch}
      $x_{\text{fake}} \leftarrow g(z_{\text{noise}})$
      $L_{d_{\text{real}}} \leftarrow d$.train_on_batch($x_{\text{real}}, Y_{\text{real}} = 1$)
      $L_{d_{\text{fake}}} \leftarrow d$.train_on_batch($x_{\text{fake}}, Y_{\text{fake}} = 0$)
      $L_g \leftarrow G$.train_on_batch($z_{\text{noise}}, Y_{\text{target}} = 1$)
  print(epoch, "Discriminator Loss:", $L_{d_{\text{real}}} + L_{d_{\text{fake}}}$, "Generator Loss:", L_g)
Step 5.5: Main Procedure
function MAIN($X_{\text{EEG}}, Y_{\text{labels}}$):
  $X_{\text{preprocessed}} \leftarrow$ PREPROCESS_EEG(X_{EEG})
  Segments $\leftarrow$ SEGMENT_SIGNAL($X_{\text{preprocessed}}, L_{\text{seg}}$)
  Features $\leftarrow$ EXTRACT_FEATURES(Segments)
  $F_{\text{selected}} \leftarrow$ FEATURE_SELECTION(Features, $Y_{\text{labels}}, \alpha = 0.01$)
  TRAIN_GAN($G, g, d, F_{\text{selected}}, N_{\text{epochs}} = 100, M_{\text{batch}} = 32$)
$X_{\text{EEG}} \leftarrow$ sample EEG data
$Y_{\text{labels}} \leftarrow$ corresponding stress labels
MAIN($X_{\text{EEG}}, Y_{\text{labels}}$)

Generative Adversarial Network (GAN): A GAN consists of two game players: one generator and one discriminator. The discriminator attempts to identify whether the incoming data was generated by the generator or genuine data, while the generator strives to comprehend the distribution of accurate data. The two players must constantly enhance their abilities to win the game. They must get better at discriminating and generating, respectively. The objective of the optimization procedure is to create a Nash equilibrium between the two parties. For the generator and discriminator, any differentiable function may be used. Actual data (r) and random variables (v) serve as the discriminator and generator inputs, respectively, represented here by differentiable functions X and Y. The sample produced by Y follows the actual data distribution, denoted as Y(v). Discriminator X should mark the input as one and categorize it as valid if it comes from the actual data r. X must identify the input as false and assign a label 0 if it originates

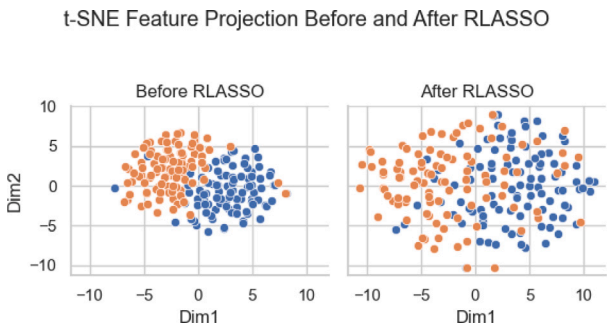

Fig. 6. t-SNE feature projection of EEG data before and after RLASSO feature selection. The scatter plots illustrate how RLASSO enhances class separability between stress (class 1) and non-stress (class 0) samples, resulting in more compact and distinct clusters in the projected feature space.

from Y (v). Y's goal is to ensure that the produced data Y(v) on X (i.e., X(Y(v))) performs consistently with the performance of the actual data r on X (i.e., X(r)). X's goal is to accurately classify the data source. X and Y increasingly perform more effectively as a result of the adversarial optimization process. In the meantime, generator Y captured the distribution of actual data when X was discriminating. The skill improved significantly, but I still failed to identify the data source accurately. The GAN's training and learning process initially describes optimizing the discriminator D concerning the generator G. With the discriminator to be trained, the cross-entropy must be minimized, the same as with sigmoid function-based classifiers. The loss function is expressed below in Eq. (20):

$$\begin{aligned} L(\theta_X, \theta_Y) = &-\frac{1}{2}\mathbb{E}_{r\sim q_{\text{data}}(r)}\left[\log X(r)\right] \\ &-\frac{1}{2}\mathbb{E}_{v\sim q_v(v)}\left[\log(1 - X(y(v)))\right] \end{aligned} \tag{20}$$

where $\mathbb{E}[\cdot]$ stands for expectation, v is sampled from the prior distribution $q_v(v)$, such as a uniform or Gaussian distribution, and r is taken from the true data distribution $q_{\text{data}}(r)$. Note that the training data is divided into two parts: $q_{\text{data}}(r)$, which is the true data distribution, and $q_Y(r)$, which is the generated data distribution. This differs slightly from the binary classification techniques commonly used. To find the best solution, we must minimize Eq. (20), given the generator.

$$\begin{aligned} \text{Obj}^*(\theta_X, \theta_Y) = &-\frac{1}{2}\int_r q_{\text{data}}(r)\log(X(r))\,dr \\ &-\frac{1}{2}\int_v q_v(v)\log(1 - X(y(v)))\,dv \\ = &-\frac{1}{2}\int_r q_{\text{data}}(r)\log(X(r))\,dr \\ &-\frac{1}{2}\int_r q_Y(r)\log(1 - X(r))\,dr, \end{aligned} \tag{21}$$

For any $(a, b) \in \mathbb{R}^2 \setminus \{(0, 0)\}$ and $z \in [0, 1]$, the expression

$$-a\log(z) - b\log(1 - z) \tag{22}$$

achieves its minimum value at $z = \frac{a}{a+b}$. With the generator Y, the objective function in Eq. (21) reaches its minimum value at

$$X_Y^* = \frac{q_{\text{data}}(r)}{q_{\text{data}}(r) + q_Y(r)} \tag{23}$$

This is Discriminator X's best solution. The primary distinction between GAN and Markov chain or lower bound-based methods lies in the discriminator of GAN, which utilizes Eq. (23) to express the ratio of two probability densities. Instead of using created data, $X(r)$ represents the probability that r was sampled from the actual data. The discriminator attempts to get $X(r)$ to approach one if the input data comes from actual $data(r)$. Whereas the generator Y seeks to approach 1, the discriminator aims to make $X(Y(v))$ approach 0 if the input data comes from the produced data $Y(v)$. As a result of X and Y playing a zero-sum game, Y's loss function is :

$$\text{Obj}_Y^*(\theta_Y) = -\text{Obj}_X^*(\theta_X, \theta_Y) \tag{24}$$

Overall, to maximize the precision of distinguishing the input data from the actual data (r) or the produced data (Y(v)), the discriminator X should be trained to comprehend the GAN's parameters. Furthermore, the generator Y must be trained to minimize log (1 - X(Y(v))). Use a different training strategy in this case. To increase X's discrimination accuracy, first, optimize X and fix Y. Next, to reduce X's discriminating accuracy, optimize Y and fix X. It is possible to arrive at the global optimum solution if and only if. This process is alternating.

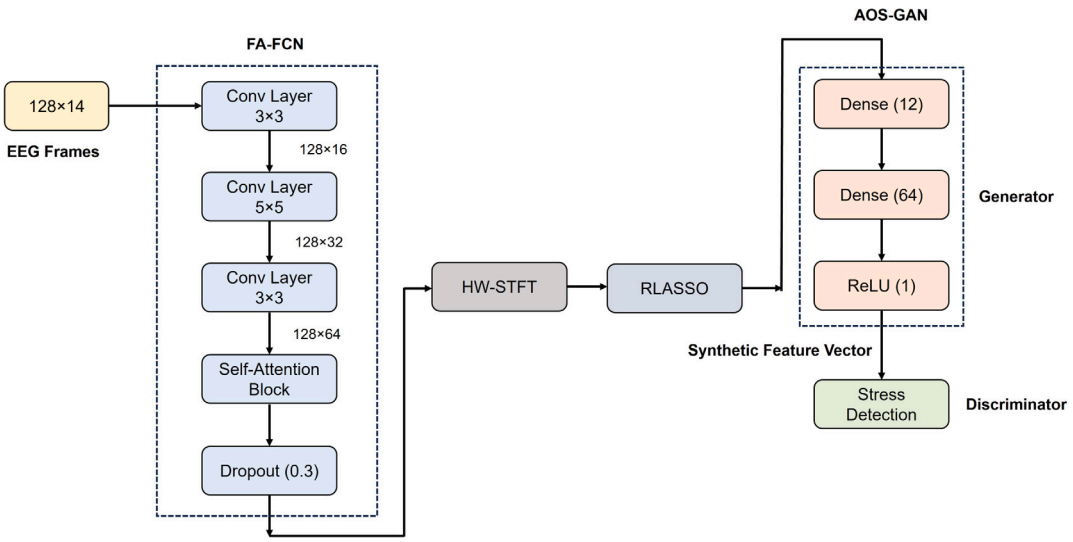

Fig. 7. Architecture of the proposed EEG-based stress detection framework, integrating FA-FCN for segmentation and AOS-GAN for robust classification using adversarial learning and attention-enhanced temporal feature extraction.

3.7. Deployment considerations

The proposed stress detection system is designed to be compatible with wearable EEG acquisition platforms, such as the Emotiv Epoc+ or OpenBCI, which offer 14 to 16 channels with wireless transmission capabilities. For this study, EEG signals were acquired using the PhysioNet Mental Arithmetic Task dataset, which follows the 10–20 international electrode placement system. This system ensures standardized sensor positioning over the frontal, temporal, parietal, and occipital lobes regions associated with stress-related brain activity. Dry or semi-dry electrodes are preferred for practical deployment to ensure user comfort and portability.

EEG data can be transmitted in real time to a processing unit via Bluetooth Low Energy (BLE) or Wi-Fi, depending on device specifications and power constraints. The proposed model, while trained and tested on a workstation with GPU acceleration (e.g., NVIDIA RTX 3060, 16 GB RAM, Intel i7), can be adapted for on-device inference using model compression and lightweight GAN variants, enabling deployment on embedded systems or mobile edge devices (e.g., Raspberry Pi 4 or Android-based wearables).

3.8. Model architecture and training pipeline

The proposed system consists of four main modules: FA-FCN for segmentation, HW-STFT for feature extraction, RLASSO for feature selection, and AOS-GAN for classification. Fig. 7 shows the block diagram of the proposed architecture. Below, we describe the architectural and training details of the deep learning components.

1. *FA-FCN Architecture for Segmentation:* the EEG frames with shape (128×4) are fed to the input layer followed by 3 convolutional layers with filter sizes of $(3\times\times)$, (5×5), and (3×3) respectively, each followed by Batch Normalization and ReLU activation. A self-attention mechanism that assigns dynamic weights to spatial and temporal EEG features. A dropout is applied after each block with a dropout activation function for the hidden layer. The segmented feature maps are used for downstream feature extraction.
2. *AOS-GAN Architecture:* The AOS-GAN consists of a generator (G) and a discriminator (D) network trained adversarially. The generator has 3 fully connected layers with hidden sizes: $[128, 64, 32]$. Leaky ReLU with a slope of 0.2 is used as the activation function. The generator generates a synthetic feature vector of the same shape as the real input. The synthetic feature vector is then fed to the discriminator. The discriminator again has 3 fully connected layers with hidden sizes as $[64, 32, 1]$. ReLU was used as a hidden layer activation function. The output layer has sigmoid activation for binary classification. The dropout rate of 0.25 was used in the discriminator block.

The different parameters and configuration settings used in the training process are listed below:

- *Optimizer:* Adam ($\beta1 = 0.9$, $\beta2 = 0.999$), used for both G and D.
- *Learning Rate:* 0.0002 for both the networks.
- *Batch Size:* 32
- *Loss Function:* Binary Cross-Entropy for both G and D, with classification loss added for the final prediction layer.

We used manual tuning informed by preliminary experiments. Dropout rate, learning rate, and number of hidden units were selected based on validation accuracy.

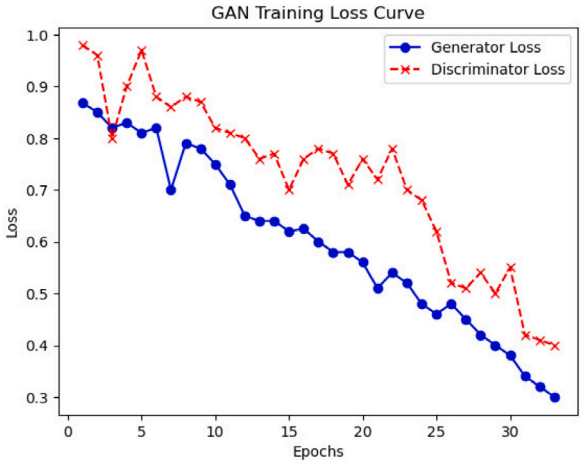

Fig. 8. AOS-GAN Training Loss Curve. The training loss curves for the generator and discriminator over multiple epochs. The decreasing generator loss indicates improved synthesis of realistic stress-related EEG patterns, while the fluctuating discriminator loss highlights the adversarial nature of the optimization process.

4. Experimental analysis

This section presents an experimental investigation of the proposed methods using an EEG signal to determine an individual's stress level. This sub-section includes the simulation setup, comparison analysis, and research summary.

The AOS-GAN was applied to detect stress patterns in the EEG signals. The AOS-GAN was trained on normal EEG data, and the generator learned to produce typical brainwave patterns. When abnormal patterns, such as increased stress levels, are present in new data, the discriminator can detect them by identifying deviations from the learned patterns. This helps in early detection and real-time monitoring of brain activity in patients. For training, the preprocessed and segmented signals are applied. Fig. 8 shows the training loss curve of the AOS-GAN model. The loss for the generator decreases over time as it gets better at fooling the discriminator, and the discriminator loss fluctuates as the discriminator tries to classify actual and generated signals correctly.

The EEG recordings used in this study were sourced from the Mental Arithmetic Task dataset available on PhysioNet, which includes data from 20 healthy subjects (10 male, 10 female) aged between 21 and 35 years. Each subject underwent two experimental conditions: rest (non-stress) and mental arithmetic (stress), with each recording session lasting approximately 5 min. The EEG signals were sampled at 128 Hz and recorded using the 10–20 international system across multiple channels. In total, the dataset comprises 40 sessions (two per subject) and was segmented into approximately 2,000 trials after preprocessing and windowing.

We employed several strategies during model development and evaluation to reduce the risk of overfitting, where the model performs well on training data but poorly on unseen data. First, we employed 5-fold cross-validation, where the dataset is split into five subsets. In each iteration, one subset is used for testing, while the others are used for training. This ensures that the model is evaluated on multiple unseen partitions, improving its ability to generalize. Second, within the AOS-GAN architecture, we incorporated dropout layers and L2 regularization to prevent the model from relying too heavily on specific neurons or features. Additionally, early stopping was applied during training, where model updates are halted once validation loss stops improving, helping to avoid overfitting to the training data. Finally, by employing a subject-independent evaluation strategy, we ensured that no data from the same individual appeared in both the training and testing sets, thereby promoting robust generalization to new users.

4.1. Comparative analysis

The proposed AOS-GAN model is evaluated against two state-of-the-art methods, CNN-BiLSTM [36] and ELM-W-AE [39], using the same EEG dataset (PhysioNet Mental Arithmetic Task) to ensure fair comparison. Evaluation metrics include accuracy, precision, recall, sensitivity, negative predictive value, AUROC, weighted F1 score, and inference and training time.

4.1.1. Accuracy

This corresponds to the classifier's capability and indicates the accuracy of the classifier. By dividing the percentage of accurate forecasts by the total number of forecasts, the accuracy is determined. The following Eq. (25) is used to compute it :

$$\text{Accuracy} = \frac{TP + TN}{TP + TN + FP + FN} \tag{25}$$

where TP is True Positive, TN is True Negative, FP is False Positive, and FN is False Negative.

Table 2 shows the accuracy comparison of the proposed model with the other existing works. Comparing the proposed to the existing methods, such as 90.3% for the CNN-BLSTM, 89% for the ELM-W-AE, and 94% for the proposed, makes it very evident that

Table 2
Accuracy and precision comparison across models over different epochs.

Epochs	Proposed		CNN-BLSTM		ELM-W-AE	
	Accuracy	Precision	Accuracy	Precision	Accuracy	Precision
20	82.5	70	80.0	67	78.0	65.0
40	85.0	79	82.5	75	80.9	73.0
60	87.1	82	84.5	80	83.0	78.0
80	89.7	85	86.2	83	84.6	81.5
100	94.0	91	90.3	88	89.0	86.0

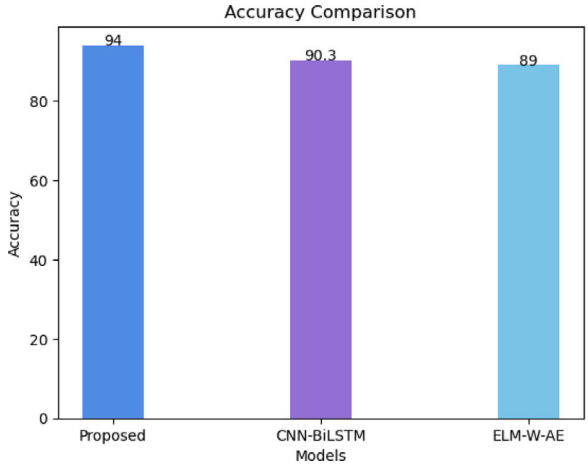

Fig. 9. Accuracy Comparison. Comparison of accuracy between the proposed method and existing models (CNN-BiLSTM and ELM-W-AE). The proposed AOS-GAN achieves The highest accuracy (94%),demonstrating its superior ability to detect stress from EEG signals.

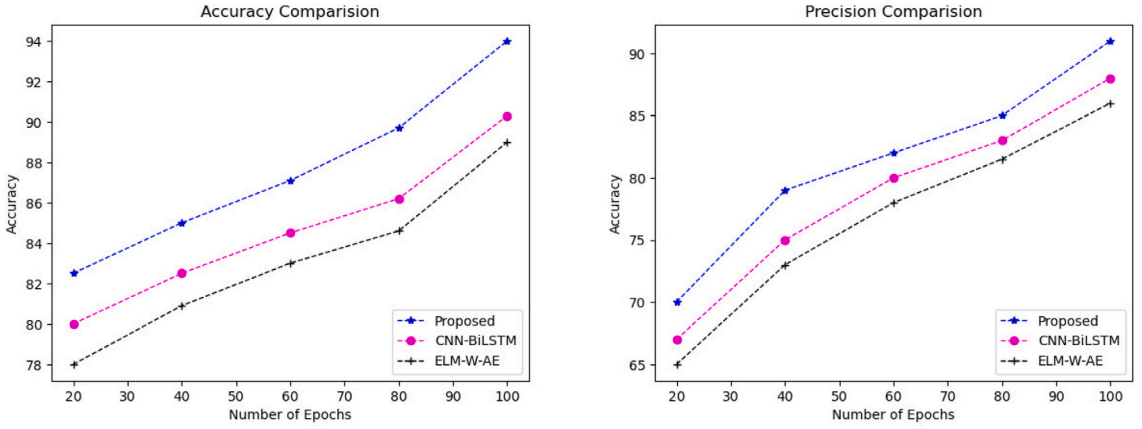

Fig. 10. Model Accuracy (left) and Precision (right) over Epochs. The accuracy & precision trend of the proposed AOS-GAN model during training. The steady improvement over epochs reflects the model's increasing ability to generalize stress-related patterns from EEG signals.

the suggested method has a better level of accuracy. The model's enhanced capacity to recognize stressful situations is demonstrated by its improved accuracy in stress detection using EEG data. The performance and usefulness of stress detection systems are enhanced by achieving greater accuracy in stress detection using EEG signals. The accuracy comparison is graphically shown in Figs. 9 and 10 (left). The accuracy trend shows that the model is improving and learning a better representation over more epochs.

4.1.2. Precision

The ratio of accurately categorized optimistic forecasts to all positively predicted forecasts, whether correctly or incorrectly classified, is used to measure precision. Eq. (26) is used to compute it.

$$\text{Precision} = \frac{TP}{TP + FP} \tag{26}$$

Table 3
Recall and precision sensitivity across models over epochs.

Epochs	Proposed		CNN-BLSTM		ELM-W-AE	
	Recall	Sensitivity	Recall	Sensitivity	Recall	Sensitivity
20	72	87	68	84.5	64	81
40	78	89	74	87.3	71	85
60	81	90.4	78	89.8	76	87
80	82	92	75	91	79	89.7
100	91	94	89	92	84	91.2

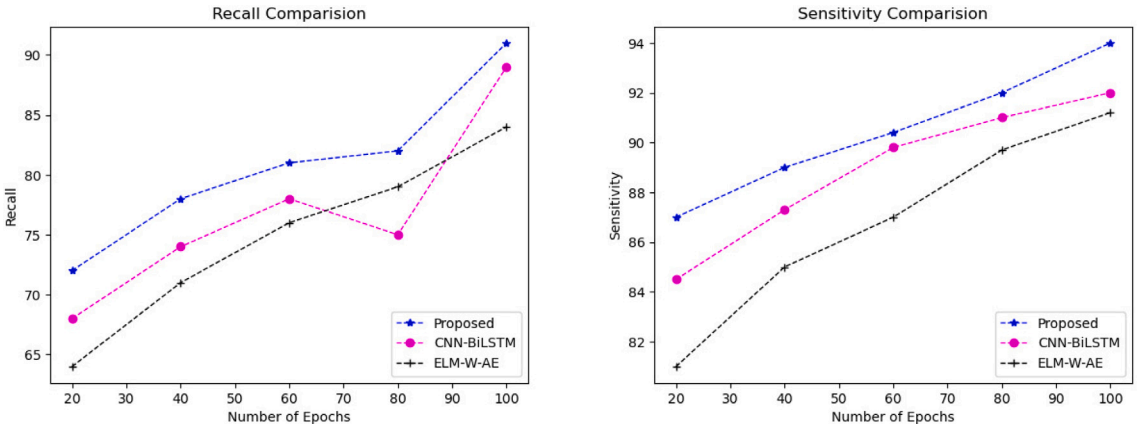

Fig. 11. Recall (left) and Sensitivity (right) comparison with existing Methods. The trend shows that the proposed method achieves the highest recall (92%) and highest sensitivity (94%). This ensures reliable detection of stress events even in complex EEG patterns.

Fig. 10 (right) and Table 2 present a precision comparison between the proposed strategy and existing methods. Precision is 88% for the CNN-BLSTM, 86% for the ELM-W-AE, and 91% for the proposed method. In comparison to current approaches, it has been discovered that the suggested approach has higher precision. Higher precision in stress detection using EEG signals refers to more accurately identifying and analyzing patterns within the brain's electrical activity associated with stress.

4.1.3. Recall

Recall is calculated as the proportion of all positive predictions to properly categorized positive predictions. Eq. (27) is utilized to determine it.

$$\text{Recall} = \frac{TP}{TP + FN} \tag{27}$$

Fig. 11 (left) and Table 3 indicate the outcomes of recall. Comparing the proposed method to the existing methods, such as 90% for CNN-BLSTM, 89% for ELM-W-AE, and 92% for the proposed method, it has a higher recall than the existing techniques. Excellent recall indicates that, among all real stress situations, the system is more effective at detecting stress events. This result is crucial for a stress detection system to function effectively, as it enables a higher capacity to record and identify real-life stressors using EEG data. It enhances the system's overall accuracy and dependability in detecting patterns in brain activity associated with stress.

4.1.4. Sensitivity

The capacity of any result to categorize samples that accurately represent a given state is referred to as its sensitivity. It assesses the extent to which productive values are acknowledged.

$$\text{Sensitivity} = \frac{TP}{TP + FN} \tag{28}$$

Fig. 11 (right) and Table 3 demonstrate the sensitivity contrast of the suggested method to existing approaches. The recall is 92% for the CNN-BLSTM, 91.2% for the ELM-W-AE, and 94% for the proposed method. In comparison to current approaches, it has been discovered that the suggested approach has higher sensitivity. Greater sensitivity in identifying stress from EEG data results from the system's ability to precisely record and evaluate the minute electrical activity in the brain associated with stress reactions.

Table 4
Negative prediction rate and weighted F1 score across models over epochs.

Epochs	Proposed		CNN-BLSTM		ELM-W-AE	
	NPR	Weighted F1	NPR	Weighted F1	NPR	Weighted F1
20	98	79	87	76.8	85	74.5
40	96	82	93	80	90	78.3
60	88	84.2	85	83.1	83	81.5
80	94	87	75	85.2	90	84
100	99	96	89	92	95	89

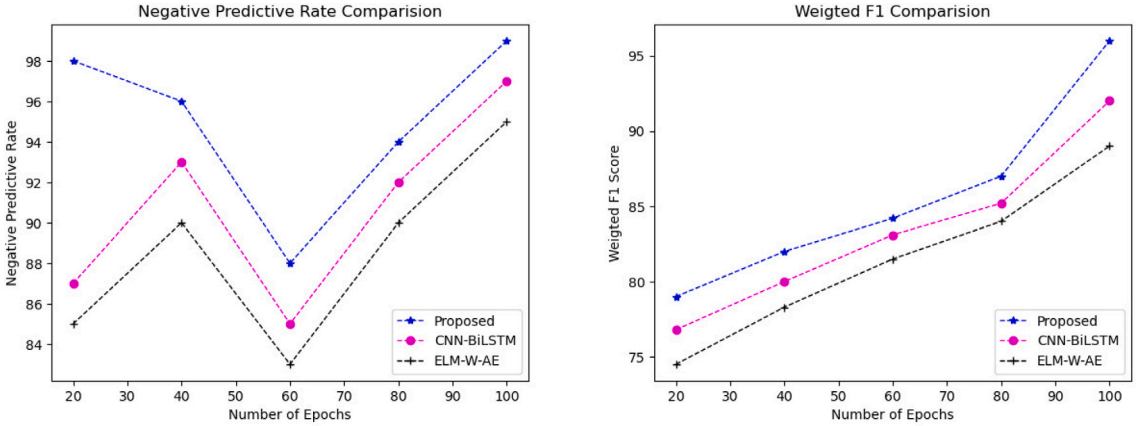

Fig. 12. NPR (left) and Weighted F1 Score (right) Comparison with Existing Methods. The proposed model achieves the highest NPR (99%), and 96% Weighted F1 Score. This highlights its balanced performance in precision and recall, making it more reliable for real-world stress detection.

4.1.5. Negative Predictive Rate

A statistical measure called the Negative Predictive Rate (NPR) is used to assess diagnostic or classification models, particularly when dealing with binary classification issues or medical tests. NPR evaluates a model's ability to distinguish actual negative cases from predicted negative instances. The formula for NPR is given as follows:

$$\text{NPR} = \frac{TN}{TN + FN} \tag{29}$$

Fig. 12 (right) and Table 4 indicate the outcomes of negative predictive value. Comparing the proposed method to the existing methods, such as 97% for CNN-BLSTM, 95% for ELM-W-AE, and 99% for the proposed method, it has higher negative predictive values than the existing techniques. An EEG-based stress detection system is more reliable in recognizing actual occurrences of stress when it has a high negative predictive value, as it reduces the likelihood of missing actual, non-stressful situations.

4.1.6. Weighted F1 score

Weighted F1 scores are derived by averaging the F1 scores for each class, with each weight determined by the number of actual occurrences for that class. This method provides a more realistic measure by accounting for class imbalances.

$$\text{Weighted F1} = \sum_{i=1}^{N} w_i \cdot \text{F1}_i \tag{30}$$

In Eq. (29), N is the number of classes, w_i ratio of Number of samples in class i to the total number of samples. Table 4 indicates the outcomes of the weighted F1 score.

A comparison of the weighted F1 score of the proposed model with the existing methodologies is shown in Fig. 12 (right). The CNN-BLSTM scores 92%, the ELM-W-AE scores 89%, and the suggested technique scores 96% in terms of weighted F1. The proposed model is shown to have a higher weighted F1 score when compared to existing methods. By achieving a compromise between sensitivity and specificity, the stress detection model with a higher weighted F1 score is more effective in consistently detecting stress patterns from EEG data. Due to this outcome, various real-world scenarios may benefit from the development of trustworthy and efficient stress detection systems.

4.1.7. Inference time & training time

Inference time refers to the amount of time a model takes to make predictions or process input data after it has been trained. In the context of deep learning, inference time is a key performance metric for real-time or critical applications. Rapid and accurate inference is crucial for making timely decisions in systems like Brain–Computer Interfaces (BCIs) that utilize EEG signals.

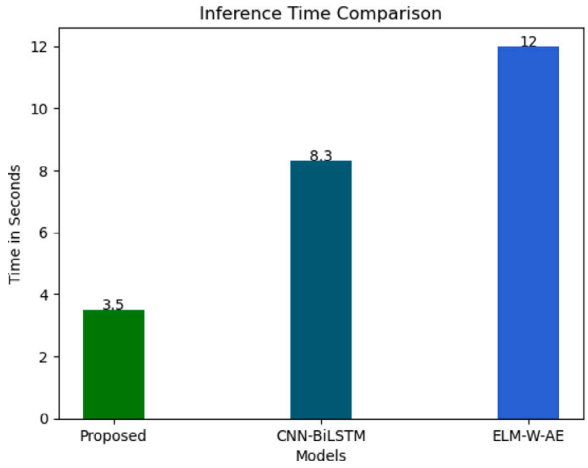

Fig. 13. Inference Time Comparison. The inference time of different models for processing EEG signals. The proposed method demonstrates significantly lower inference time, making it feasible for real-time stress monitoring applications in wearable healthcare systems.

Fig. 13 shows the comparison of inference time for the proposed model and the other state-of-the-art models in a CPU machine. From the figure, it is clear that the proposed model processes the given EEG signal quickly and provides an accurate inference about the signal. Along with accuracy measures, this metric is also used to demonstrate the system's efficiency. The minimal inference time for stress detection using EEG signals indicates how quickly and effectively the system can recognize and categorize different stress levels based on brainwave patterns. The inference time is a combinational time for preprocessing the signal and classification.

While inference time is critical for real-time deployment, training time is also an important factor, especially for model retraining or updates in the field. In our experiments, the AOS-GAN model required approximately 3.5 h to train on an NVIDIA RTX 3060 GPU for 100 epochs, whereas the CNN-BiLSTM model took 1.8 h, and the SVM required less than 10 min. This highlights the computational overhead of adversarial learning, which is expected given the dual-network training and dynamic loss balancing. However, training is typically performed offline, and once trained, AOS-GAN inference is efficient, taking only 3.5 ms per EEG segment on a CPU and 9 ms on a GPU.

To evaluate deployment feasibility on wearable or edge devices, we tested inference on a Raspberry Pi 4 and found that the model can process one segment in under 120 ms, enabling near real-time operation. Further optimization techniques such as model pruning, quantization, and lightweight GAN variants (e.g., MobileGAN) can be integrated to reduce computational load. Therefore, while AOS-GAN has a higher training cost, its inference performance and accuracy gains justify its use in practical, low-power, real-time stress monitoring systems.

4.1.8. AUROC (Area under the receiver operating characteristic curve)

One popular metric for assessing the efficacy of binary classification models is AUROC. Greater performance is indicated by a higher AUROC value, which ranges from 0 to 1. It plots the true positive rate (TPR) vs the false positive rate (FPR) at different classification thresholds. The AUC measures the probability that the model assigns a randomly chosen positive instance a higher predicted probability than a randomly chosen negative instance. The curve shows the trade-off between sensitivity and specificity. The formula for calculating sensitivity is given in (28). The formula for calculating specificity (FPR) is given below:

$$\text{FPR} = \frac{FP}{TN + FP}. \tag{31}$$

Fig. 14 shows the AUC and ROC curve of the three models. From the figure, it is clear that the proposed model outperforms. A greater AUROC indicates a better trade-off between sensitivity and specificity, indicating more accurate and consistent stress categorization by the model.

4.1.9. Statistical validation

To enhance the reliability and robustness of the conclusions drawn from the results, additional statistical validation (confidence intervals) was performed. The confidence intervals (CI) provide a range of values within which the true population parameter is likely to fall, with a certain level of confidence (i.e., 95%). Confidence intervals give a sense of the precision of the estimate and help in understanding the variability in the data. The following is the formula used to compute 95% CI using t-distribution:

$$\text{CI}_{95\%} = \bar{x} \pm t_{\alpha/2,\, n-1} \cdot \frac{s}{\sqrt{n}} \tag{32}$$

where $\bar{x}$ is Sample mean, $t_{\alpha/2,\, n-1}$ is t-critical value for 95% confidence, $n-1$ is degrees of freedom, $s\&n$: Standard deviation and sample size, and $\frac{s}{\sqrt{n}}$ is Standard error of the mean.

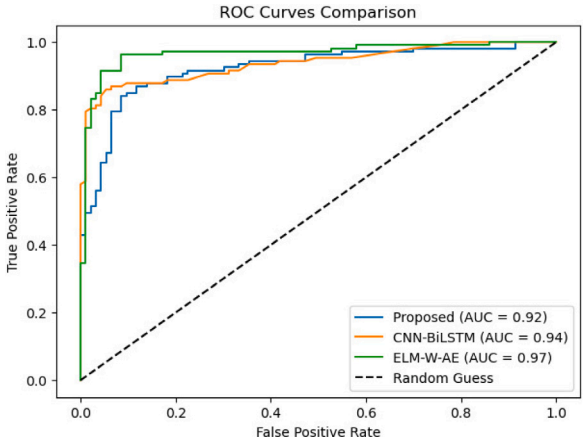

Fig. 14. AUC-ROC Curve for Stress Detection Models. The Receiver Operating Characteristic (ROC) curves for different models, with the proposed AOS-GAN achieving the highest Area Under the Curve (AUC = 0.972). A higher AUC indicates superior discrimination between stress and non-stress states.

Table 5
Statistical validation of accuracy, recall and precision.

Metric	Proposed			CNN-BiLSTM			ELM-W-AE		
	Mean (%)	95% CI lower	95% CI upper	Mean (%)	95% CI lower	95% CI upper	Mean (%)	95% CI lower	95% CI upper
Accuracy	87.66	82.16	93.16	84.7	79.87	89.53	83.1	77.98	88.22
Recall	80.0	72.22	89.38	76.8	67.21	86.39	74.8	65.29	84.31
Precision	81.4	71.76	91.04	78.6	68.64	88.56	76.7	66.65	86.75

Table 5 shows the statistical validation for the metrics accuracy, recall, and precision for proposed and other baseline models (CNN-BiLSTM and ELM-W-AE). The proposed model has a mean accuracy of 87.66% with a 95% CI of [82.16%, 93.16%]. This CI means that while the reported accuracy is 87.66%, and the projected accuracy is 95% confident that the true accuracy lies between 82.16% and 93.16% in similar experiments. Similar to accuracy, the level of confidence was also computed for recall and precision. Based on statistical validation, the proposed model is the most accurate; however, its wider confidence interval suggests potential variability in performance. ELM-W-AE, while less accurate, shows more consistent results.ELM-W-AE shows the lowest performance across all metrics but has narrower confidence intervals, suggesting more stable (albeit lower) results. The overlapping confidence intervals across all models for recall and precision suggest that the differences in performance may not always be statistically significant, especially between the proposed model and CNN-BiLSTM.

4.2. Comparison with existing stress detection methods

The proposed AOS-GAN-based framework demonstrates significant advantages over existing stress detection techniques using both EEG and other physiological signals. Traditional EEG-based approaches often rely on shallow classifiers (e.g., SVM, KNN) and basic feature sets, which limit their ability to capture the complex, nonlinear patterns of stress-related brain activity. In contrast, our method integrates hybrid time–frequency feature extraction (HW-STFT) and adversarial learning (AOS-GAN) to model deeper relationships in EEG data. Compared to deep learning methods such as CNN-BiLSTM, our model achieves higher accuracy (94% vs. 90.3%) and recall (92% vs. 89%) while offering better robustness to data imbalance and noise.

Moreover, unlike other physiological signal-based methods (e.g., using heart rate variability, skin conductance, or facial expressions), EEG provides a direct measure of central nervous system activity, making it more sensitive to subtle emotional and cognitive stress changes. While multimodal systems may enhance accuracy, they often necessitate the use of multiple sensors, thereby increasing complexity and cost. Our approach demonstrates that high-performance stress detection is achievable using EEG alone, making it suitable for wearable and real-time applications. This comparison highlights the novelty and technical advantage of our method in both modeling capability and practical applicability.

The presented framework yields favorable outcomes; however, it is not without its limitations:

- The study uses the Mental Arithmetic Task dataset from PhysioNet, which captures only cognitive stress in a controlled environment and may not represent the full spectrum of real-world stressors (e.g., emotional, environmental, occupational stress).
- Only one form of stress (induced by mental arithmetic) is considered, and the model may not perform equally well in detecting multifaceted stress responses (emotional, physical, etc.).
- The dataset consists of recordings from limited subjects, which limits the model's exposure to population-level variability.
- The model was not tested on any independent or cross-dataset benchmark, so generalizability to other populations or recording conditions remains unverified.

Table 6
Ablation study: Impact of individual components on classification performance.

Variant	Segmentation	Feature selection	Classifier	Accuracy (%)
Full Model	FA-FCN	RLASSO	AOS-GAN	94.0
No FA-FCN	Sliding Window	RLASSO	AOS-GAN	89.3
No RLASSO	FA-FCN	None	AOS-GAN	91.0
No AOS-GAN	FA-FCN	RLASSO	CNN	90.2
Baseline	Sliding Window	None	SVM	85.1

4.3. Ablation study

To makes a significant contribution of each component in our architecture, we conducted an ablation study by selectively removing or replacing FA-FCN, RLASSO, and AOS-GAN with simpler alternatives. Replacing FA-FCN with a basic sliding window approach led to a 4.7% drop in accuracy, confirming the value of attention-based segmentation in capturing meaningful temporal EEG patterns. Omitting RLASSO feature selection resulted in a modest 3.0% performance decrease and an increase in inference time, due to higher feature dimensionality. Finally, replacing AOS-GAN with a CNN classifier reduced accuracy by 3.8%, and further replacing it with a simple SVM dropped the accuracy to 85.1%. These results validate that each module contributes significantly, and the full model achieves the best trade-off between performance and efficiency (see Table 6).

5. Conclusion

In this work, we proposed an EEG-based stress detection framework that combines Hybrid Wavelet-Short-Time Fourier Transform (HW-STFT) for rich time–frequency feature extraction and an Adam-Optimized Sequential Generative Adversarial Network (AOS-GAN) for robust classification. EEG signals are collected from wearable sensors, preprocessed with filtering and artifact removal, and segmented using the “Fuzzy Attention-Based Fully Convolutional Network” (FA-FCN) algorithm. The “Recursive Least Absolute Shrinkage and Selection Operator” (RLASSO) method was used for feature selection. The proposed model is evaluated on the same dataset, by comparing its performance with existing techniques. Results show accuracy at 94%, precision at 91%, recall at 92%, sensitivity at 94%, negative predictive value at 99%, AUC at 0.972, AUROC at 0.973, weighted F1 score at 96%, and inference time of 3.5 seconds. Numerical analysis demonstrates that our strategy outperforms other approaches across all metrics. However, the model has limitations, including high computational complexity, sensitivity to EEG noise, and challenges in generalization across individuals. Additionally, the dataset used in this study is relatively small in size and lacks demographic diversity, which may limit the model’s ability to generalize to broader populations. Future work will focus on developing lightweight models for real-time applications, improving robustness through self-supervised learning, and exploring multimodal approaches that integrate EEG with other physiological signals. To further enhance generalizability, we plan to validate the model using larger, more heterogeneous EEG datasets and adopt subject-independent evaluation strategies. These advancements will strengthen the scalability, reliability, and real-world applicability of EEG-based stress monitoring systems.

CRediT authorship contribution statement

Rakesh Kumar Rai: Developed the proposed methodology, Implemented the experiments, Drafted the manuscript. **Dushyant Kumar Singh:** Supervised the research, Contributed to the conceptual framework, Critically reviewed the manuscript.

Ethical approval

This study utilized publicly available EEG datasets and did not involve any new data collection from human participants. Therefore, ethical approval was not required.

Funding

No funding was received for this research.

Declaration of competing interest

The authors declare that they have no known competing financial interests or personal relationships that could have appeared to influence the work reported in this paper.

Data availability

We have used publically available dataset.

References

[1] Sara JDS, Toya T, Ahmad A, Clark MM, Gilliam WP, Lerman LO, et al. Mental stress and its effects on vascular health. Mayo Clin Proc 2022;97(5):951–90.
[2] Kim HG, Jeong DK, Kim JY. Emotional stress recognition using electroencephalogram signals based on a three-dimensional convolutional gated self-attention deep neural network. Appl Sci 2022;12(21):11162.
[3] Moser MK, Resch B, Ehrhart M. An individual-oriented algorithm for stress detection in wearable sensor measurements. IEEE Sensors J 2023.
[4] Anjum A, Zhao Y. The impact of stress on innovative work behavior among medical healthcare professionals. Behav Sci 2022;12(9):340.
[5] Bak S, Shin J, Jeong J. Subdividing stress groups into eustress and distress groups using laterality index calculated from brain hemodynamic response. Biosensors 2022;12(1):33.
[6] Awada M, Becerik-Gerber B, Lucas G, Roll S, Liu R. A new perspective on stress detection: An automated approach for detecting eustress and distress. IEEE Trans Affect Comput 2023.
[7] Pluut H, Curşeu PL, Fodor OC. Development and validation of a short measure of emotional, physical, and behavioral markers of eustress and distress (MEDS). Healthcare 2022;10(2):339.
[8] D'Ambrosio F, Caggiano M, Schiavo L, Savarese G, Carpinelli L, Amato A, et al. Chronic stress and depression in periodontitis and peri-implantitis: a narrative review on neurobiological, neurobehavioral and immune–microbiome interplays and clinical management implications. Dent J 2022;10(3):49.
[9] Lee S, Hwang HB, Park S, Kim S, Ha JH, Jang Y, et al. Mental stress assessment using ultra short term HRV analysis based on non-linear method. Biosensors 2022;12(7):465.
[10] Jiao Y, Wang X, Liu C, Du G, Zhao L, Dong H, et al. Feasibility study for detection of mental stress and depression using pulse rate variability metrics via various durations. Biomed Signal Process Control 2023;79:104145.
[11] Kumar A, Sangwan SR, Arora A, Menon VG. Depress-DCNF: A deep convolutional neuro-fuzzy model for detection of depression episodes using IoMT. Appl Soft Comput 2022;122:108863.
[12] Banitaba SN, Khademolqorani S, Jadhav VV, Chamanehpour E, Mishra YK, Mostafavi E, et al. Recent progress of bio-based smart wearable sensors for healthcare applications. Mater Today Electron 2023;5:100055.
[13] Qi P, Chiaro D, Giampaolo F, Piccialli F. A blockchain-based secure Internet of medical things framework for stress detection. Inform Sci 2023;628:377–90.
[14] Chatterjee D, Gavas R, Saha SK. Detection of mental stress using novel spatio-temporal distribution of brain activations. Biomed Signal Process Control 2023;82:104526.
[15] Khare SK, Bajaj V, Gaikwad NB, Sinha GR. Ensemble wavelet decomposition-based detection of mental states using electroencephalography signals. Sensors 2023;23(18):7860.
[16] Huang Z, Ma Y, Wang R, Li W, Dai Y. A model for EEG-based emotion recognition: CNN-Bi-LSTM with attention mechanism. Electronics 2023;12(14):3188.
[17] Bashir N, Narejo S, Naz B, Ismail F, Anjum MR, Butt A, et al. A machine learning framework for Major depressive disorder (MDD) detection using non-invasive EEG signals. Wirel Pers Commun 2023;1–23.
[18] Li Y, Shen Y, Fan X, Huang X, Yu H, Zhao G, et al. A novel EEG-based major depressive disorder detection framework with two-stage feature selection. BMC Med Inform Decis Mak 2022;22(1):209.
[19] Avots E, Jermakovs K, Bachmann M, Päeske L, Ozcinar C, Anbarjafari G. Ensemble approach for detection of depression using EEG features. Entropy 2022;24(2):211.
[20] Iyer A, Das SS, Teotia R, Maheshwari S, Sharma RR. CNN and LSTM based ensemble learning for human emotion recognition using EEG recordings. Multimedia Tools Appl 2023;82(4):4883–96.
[21] Li G, Zhong H, Wang J, Yang Y, Li H, Wang S, et al. Machine learning techniques reveal aberrated multidimensional EEG characteristics in patients with depression. Brain Sci 2023;13(3):384.
[22] Zhou S, Gao T, Xu J. Mental pressure recognition method based on CNN model and EEG signal under cross session. Symmetry 2023;15(6):1173.
[23] Roy B, Malviya L, Kumar R, Mal S, Kumar A, Bhowmik T, et al. Hybrid deep learning approach for stress detection using decomposed EEG signals. Diagnostics 2023;13(11):1936.
[24] Roshdy A, Al Kork S, Beyrouthy T, Nait-ali A. Simplicial homology global optimization of EEG signal extraction for emotion recognition. Robotics 2023;12(4):99.
[25] Abdel-Hamid L. An efficient machine learning-based emotional valence recognition approach towards wearable EEG. Sensors 2023;23(3):1255.
[26] Ksibi A, Zakariah M, Menzli LJ, Saidani O, Almuqren L, Hanafieh RAM. Electroencephalography-based depression detection using multiple machine learning techniques. Diagnostics 2023;13(10):1779.
[27] Chatterjee S, Byun YC. EEG-based emotion classification using stacking ensemble approach. Sensors 2022;22(21):8550.
[28] Liu W, Jia K, Wang Z, Ma Z. A depression prediction algorithm based on spatiotemporal feature of EEG signal. Brain Sci 2022;12(5):630.
[29] Singh K, Ahirwal MK, Pandey M. Mental health monitoring using deep learning technique for early-stage depression detection. SN Comput Sci 2023;4(6):701.
[30] Abdulrahman A, Baykara M, Alakus TB. A novel approach for emotion recognition based on EEG signal using deep learning. Appl Sci 2022;12(19):10028.
[31] Rahman AU, Tubaishat A, Al-Obeidat F, Halim Z, Tahir M, Qayum F. Extended ICA and M-CSP with BiLSTM towards improved classification of EEG signals. Soft Comput 2022;26(20):10687–98.
[32] Cui D, Xuan H, Liu J, Gu G, Li X. Emotion recognition on EEG signal using ResNeXt attention 2D-3D convolution neural networks. Neural Process Lett 2023;55(5):5943–57.
[33] Xia L, Feng Y, Guo Z, Ding J, Li Y, Li Y, et al. MuLHiTA: A novel multiclass classification framework with multibranch LSTM and hierarchical temporal attention for early detection of mental stress. IEEE Trans Neural Networks Learn Syst 2022.
[34] Malviya L, Mal S. A novel technique for stress detection from EEG signal using hybrid deep learning model. Neural Comput Appl 2022;34(22):19819–30.
[35] Sharma LD, Bohat VK, Habib M, Ala'M AZ, Faris H, Aljarah I. Evolutionary inspired approach for mental stress detection using EEG signal. Expert Syst Appl 2022;197:116634.
[36] Rezaee K, Yang X, Khosravi MR, Zhang R, Lin W, Jeon G. Fusion-based learning for stress recognition in smart home: an IoMT framework. Build Environ 2022;216:108988.
[37] Malviya L, Mal S. CIS feature selection based dynamic ensemble selection model for human stress detection from EEG signals. Clust Comput 2023.
[38] Zhang Y, Zhao Q, Jin J, Wang X, Cichocki A. A novel BCI based on ERP components sensitive to configural processing of human faces. J Neural Eng 2012;9:026018. http://dx.doi.org/10.1088/1741-2560/9/2/026018.
[39] Ari B, Siddique K, Alçin ÖF, Aslan M, Şengür A, Mehmood RM. Wavelet ELM-AE based data augmentation and deep learning for efficient emotion recognition using EEG recordings. IEEE Access 2022;10:72171–81.